Capillary force method to improve the green density of binder jet additive manufacturing

Emrecan Soylemez
Department of Mechanical Engineering, Istanbul Technical University, Istanbul, Türkiye
E-mail: *esoylemez@itu.edu.tr*

Received 14 March 2023; accepted 25 May 2023; published online 25 June 2023
DOI https://doi.org/10.21595/amr.2023.23275

Abstract. This study investigates the impact of capillary adhesion force on the green part density in metal powder binder jetting 3D printing. Gas atomized Co-Cr-Mo, SS316L, and pure Cu powders were used to print various samples. The printed samples were then treated with water, 1-Hexanol, and n-Amyl alcohol vapor for 24 hours to nucleate capillary bridges between particles and shrink samples uniformly. The volume change was calculated for each sample, and up to –3.1 % volume change was observed. The proposed method can be used to improve green part densities directly on printed parts before sintering.

Keywords: additive manufacturing, binder jet additive manufacturing, capillary bridge, capillary adhesion.

1. Introduction

Metal additive manufacturing (AM) has been integrated to the industry for medium scale production providing superior functionalities with complex part design capability while trying to be cost-competitive to conventional manufacturing. Powder bed fusion AM processes are mostly used additive manufacturing methods, and these processes use either laser or electron beam to scan the fusing area on each layer. The speed of fusion-based processes is restricted by the physics of metal melting and cooling, and they often necessitate support structures, resulting in increased production time and material wastage. Binder jet additive manufacturing (BJAM) on the other hand provides an alternative method for powder-based AM by printing parts with jetted binder droplets. Then, printed green parts are sintered to achieve the full density of the metal parts.

Binder jet additive manufacturing can provide multiple nozzles with multiple inkjet heads to cover large print areas with a single pass, and that can increase the building rates order of magnitude higher compared to powder bed fusion (PBF) processes [1]. Therefore, cost competitive industries such as the automotive and electrical industries prefer focusing on BJAM [2], [3]. The main bottleneck in the process occurs during the post-processing step, particularly during sintering. Although binder jet printing is a support free process, supports are needed to keep the form of the part at high temperatures during sintering. Pores close during sintering, and ~15-20 % shrinkage is experienced while reaching to full density [4]. Reducing the shrinkage ratio improves the process capability and reduces the distortions during sintering. Thus, green part density needs to be as high as possible to make the BJAM a reliable process.

Process parameters such as layer thickness and binder saturation play an important role in green density results [5]. Bimodal powder usage also improves green part density [6]. Powder spreading mechanisms [7] and spreading parameters [8] are also critical to change the green densities.

In this study, capillary adhesion force was proposed to improve the green part density in a unique way. Any improvement in green part density will reduce the shrinkage rate and distortion amount, and it may also improve the final part density. Three different printed parts' green densities were compared in dry conditions and after holding in vapor of water, 1-Hexanol, n-Amyl alcohol at saturated partial pressure, $\frac{p}{p_s} < 100\%$.

2. Materials and methods

2.1. Capillary adhesion

Liquid bridges between contacting spherical particles form when condensable undersaturated vapor is released to the environment [9]. Liquid bridge forms in curved meniscus shape induces a pressure difference across the liquid-vapor interface. This pressure difference is explained by the Laplace equation [10], [11]:

$$\Delta P = \frac{\gamma_L}{r_K}, \tag{1}$$

where, r_K equals the Kelvin radius, and γ_L is the surface tension of the liquid [12]. Asperity contact mechanisms are modeled as a sphere-flat surface interaction, as shown in Fig. 1. The Kelvin equation is derived using thermodynamics and the Young-Laplace equation [9]. After derivation, the Kelvin equation [11]:

$$r_K = \frac{\gamma_L V_m}{R_g T \ln(p/p_s)}, \tag{2}$$

where R_g is ideal gas constant, T is temperature, V_m is constant molar volume of the liquid substance, p is the vapor pressure, and p_s is the saturated vapor pressure.

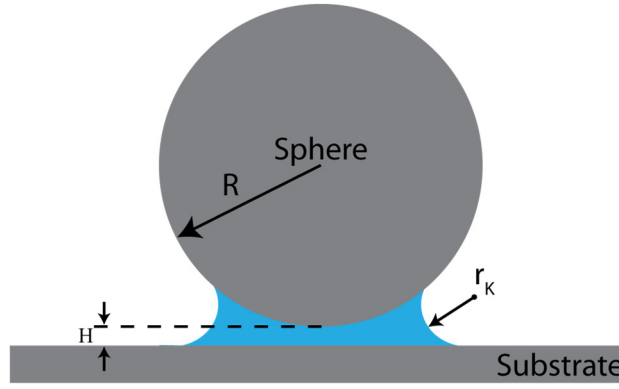

Fig. 1. Schematic of a sphere and a flat surface. $H_c = 2r_K$ is the range of the constant Laplace pressure while H is the gap between two facing bodies

For a sphere-flat geometry, assuming that the sphere particle radius R is much larger than $|r_K|$. The capillary force F_c under thermodynamic equilibrium can be found from the Laplace and Kelvin equations as [12]:

$$F_c = -4\pi R\gamma_L \cos\theta \left[1 - \frac{H}{2|r_K|}\right], \tag{3}$$

where, θ is the contact angle between the meniscus and the surface, and H denotes the separation between two bodies. The simplified calculation of capillary force is suitable for the interaction between metal powder particles due to r_K range being in the nanometer scale, whereas the average diameter of metal particles is ~15 – 30 μm. Capillary adhesion force interpretated as the force that pulls particles in green parts closer to each other.

Three different liquid bridge effects were tested using water, 1-Hexanol, and n-Amyl alcohol. Their surface tension and r_K values at p/p_s = 0.9 and room temperature are given in Table 1 [13],

[14]. Water was chosen for its high surface tension, which results in a high capillary force value. 1-Hexanol and n-Amyl alcohol were selected for their long liquid bridges, which enable more interactions between particles with larger gaps in between.

Table 1. Water, 1-Hexanol, and n-Amyl alcohol surface tension, molar volume and calculated Kelvin radius at 0.9 partial pressure

Solution	γ (N/m)	V_m (l/mol)	r_K (nm)
water	0.073	0.018	5.0
1-Hexanol	0.025	0.124	11.6
n-Amyl alcohol	0.026	0.108	10.7

2.2. Binder jet additive manufacturing

The gas atomized powders of Co-Cr-Mo, SS316L, and pure Cu were used to print various samples. The powder morphologies were investigated by scanning electron microscopy, as shown in Fig. 2. Particle size distribution of the powders was measured using a laser diffraction particle size analyzer, and the volumetric size distributions were plotted in Fig. 3. The median diameter (D50) for Co-Cr-Mo, SS316L and Cu was 33 µm, 17 µm and 20 µm, respectively.

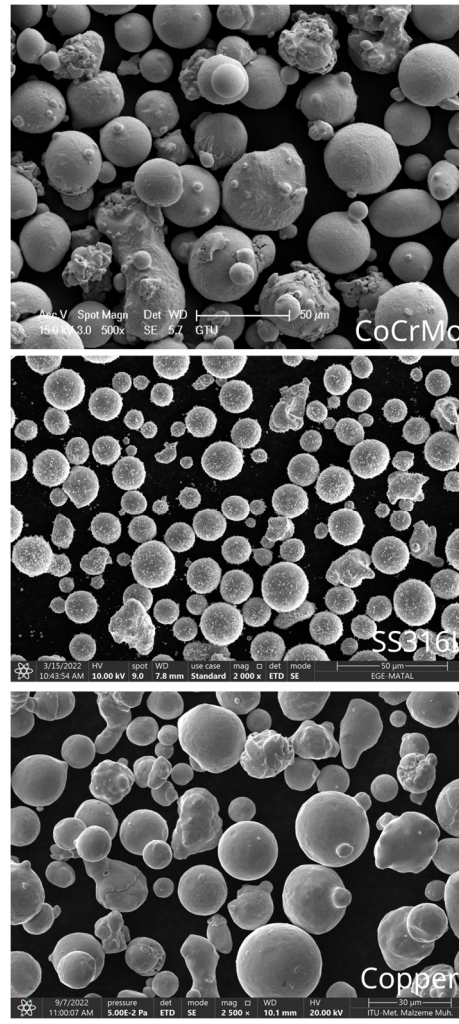

Fig. 2. Scanning electron microscope images of CoCrMo, SS316L, and Cu powders

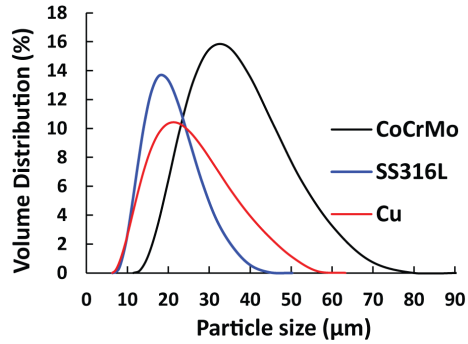

Fig. 3. Particle size distributions of CoCrMo, SS316L, and Cu powders

The binder jetting samples were obtained using Sinterjet printer (more details in [15]). Available printed parts were used in this study with various powders to differentiate the response with different materials. Therefore, 6×7×8 mm prisms, 4×10×10 mm prisms and 6×10×10 mm prisms were used for Co-Cr-Mo, SS316L, and pure Cu, respectively. All printed samples were at ~50 % relative green density after print.

2.3. High partial pressure vapor experiments

Printed samples were subjected to treatment in water, 1-Hexanol, and n-Amyl alcohol vapor for 24 hours, with three samples being treated for each vapor condition. A cotton piece soaked in the liquid was placed with the samples sitting on zirconia beads to eliminate friction effect, as seen in Fig. 4 in the zip lock. After 24-hour soaking period, samples were left in air for another 24-hour period. The dimensions of each sample were measured before and after treatment using a caliper with a 0.01 mm resolution.

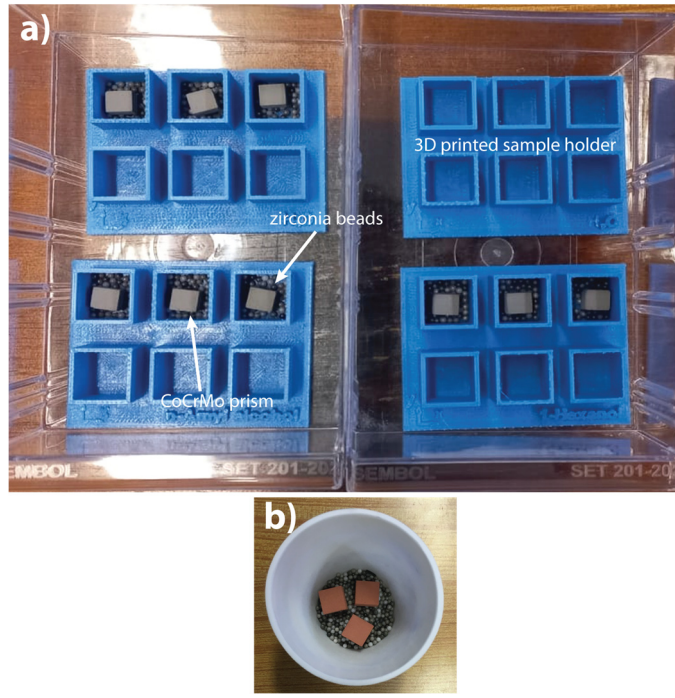

Fig. 4. Rectangular prism green parts experimental sample holders a) CoCrMo and b) Cu. Both holders provide the same condition. a) helps keeping the order of the samples

3. Results

Volume change were calculated for each sample and plotted in Fig. 4. The circle markers correspond to water treatment, which resulted in a –3.1 % volume change for Co-Cr-Mo. On the other hand, 1-Hexanol and n-Amyl alcohol treatments resulted in an average volume change of -1.46 % and –1.82 %, respectively. The use of Water for copper powder also resulted in larger green densities, as seen in Fig. 4. However, SS316L exhibited the lowest volume change in response to water. Eq. (3), capillary force calculation results with larger force values as surface tension increases from alcohols to water in our case, and capillary bridge can nucleate in $2\times r_K$ range between facing surfaces. It is possible that the higher liquid bridges provided by 1-Hexanol and n-Amyl alcohol may have caused a larger adhesive force compared to water.

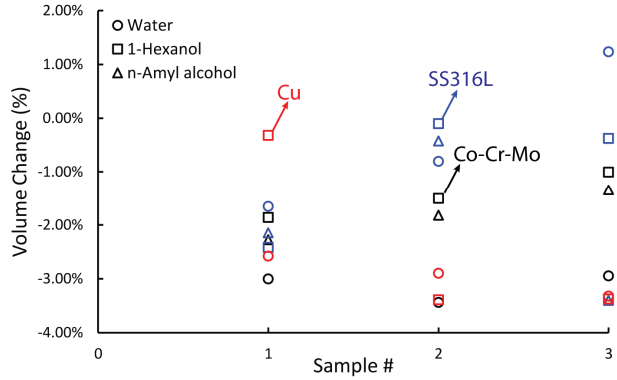

Fig. 5. Rectangular prism green parts volume change results for each sample treated in vapor of water, 1-Hexanol, and n-Amyl alcohol. Different color represents different material, and different marker represents different vapor treatment. (Copper samples were not soaked in n-Amyl alcohol; thus, no data plotted)

SS316L has the narrowest PSD and the smallest median particle size. Narrow PSD may cause the particles spread further apart, and that may need larger capillary bridges to nucleate. In all cases, on average volume changes were observed to be between –0.41 % and –3.13 %.

4. Conclusions

Capillary adhesion force effect on green part density was tested. Water, 1-Hexanol, and n-Amyl alcohol vapor were used to nucleate capillary bridges between particles to shrink samples uniformly before sintering. Up to –3.1 % volume change was observed.

This proposed method can be used to improve green part densities. It complies with other methods to improve the green densities because it can be used directly to the printed parts right before sintering. Further research should be conducted to see the effectiveness at complex parts. Also, distortion comparisons after sintering need to be studied in future work.

Acknowledgements

The authors have not disclosed any funding.

Data availability

The datasets generated during and/or analyzed during the current study are available from the corresponding author on reasonable request.

Conflict of interest

The authors declare that they have no conflict of interest.

References

[1] A. M. Elliott, C. L. Cramer, P. Nandwana, M. Chmielus, and A. Mostafaei, "Binder Jet-Metals," *Reference Module in Materials Science and Materials Engineering*, Vol. 1, 2021.

[2] Michael Freeman, "Overcoming cost barriers of metal-binder-jet additive-manufacturing for automotive product applications," 2022.

[3] "GKN additive to showcase award-winning metal binder jetting mass production capabilities at Formnext 2022." GKN Powder Metallurgy. https://www.gknpm.com/en/news-and-media/news-releases/2022/gkn-additive-to-showcase-award-winning-metal-binder-jetting-mass-production-capabilities-at-formnext-2022/ (accessed 2022).

[4] M. Li, W. Du, A. Elwany, Z. Pei, and C. Ma, "Metal binder jetting additive manufacturing: A literature review," *Journal of Manufacturing Science and Engineering*, Vol. 142, No. 9, pp. 1–17, Sep. 2020, https://doi.org/10.1115/1.4047430

[5] S. Bafaluy Ojea, J. Torrents-Barrena, M. T. Pérez-Prado, R. Muñoz Moreno, and F. Sket, "Binder jet green parts microstructure: advanced quantitative analysis," *Journal of Materials Research and Technology*, Vol. 23, pp. 3974–3986, Mar. 2023, https://doi.org/10.1016/j.jmrt.2023.02.051

[6] Y. Bai, G. Wagner, and C. B. Williams, "Effect of particle size distribution on powder packing and sintering in binder jetting additive manufacturing of metals," *Journal of Manufacturing Science and Engineering*, Vol. 139, No. 8, p. 08101, Aug. 2017, https://doi.org/10.1115/1.4036640

[7] S. Cao, Y. Qiu, X.-F. Wei, and H.-H. Zhang, "Experimental and theoretical investigation on ultra-thin powder layering in three dimensional printing (3DP) by a novel double-smoothing mechanism," *Journal of Materials Processing Technology*, Vol. 220, pp. 231–242, Jun. 2015, https://doi.org/10.1016/j.jmatprotec.2015.01.016

[8] P. S. Desai and C. F. Higgs, "Spreading process maps for powder-bed additive manufacturing derived from physics model-based machine learning," *Metals*, Vol. 9, No. 11, p. 1176, Oct. 2019, https://doi.org/10.3390/met9111176

[9] A. W. Adamson and A. P. Gast, *Physical Chemistry of Surfaces*. Wiley, 1997.

[10] J. Israelachvili, *Intermolecular and Surface Forces*. Academic Press, 1985.

[11] W. Thomson, "On the equilibrium of vapour at a curved surface of liquid.," *Proceedings of the Royal Society of Edinburgh*, Vol. 7, p. 63, 1870.

[12] M. P. de Boer and P. C. T. de Boer, "Thermodynamics of capillary adhesion between rough surfaces," *Journal of Colloid and Interface Science*, Vol. 311, No. 1, pp. 171–185, Jul. 2007, https://doi.org/10.1016/j.jcis.2007.02.051

[13] E. Soylemez and M. P. de Boer, "Crack healing between rough polycrystalline silicon hydrophilic surfaces in n-pentanol and water vapors," *Tribology Letters*, Vol. 59, No. 1, pp. 1–12, Jul. 2015, https://doi.org/10.1007/s11249-015-0525-2

[14] E. Jiménez, H. Casas, L. Segade, and C. Franjo, "Surface tensions, refractive indexes and excess molar volumes of hexane+1-alkanol mixtures at 298.15 K," *Journal of Chemical and Engineering Data*, Vol. 45, No. 5, pp. 862–866, 2000.

[15] R. Onler, A. S. Koca, B. Kirim, and E. Soylemez, "Multi-objective optimization of binder jet additive manufacturing of Co-Cr-Mo using machine learning," *The International Journal of Advanced Manufacturing Technology*, Vol. 119, No. 1-2, pp. 1091–1108, Mar. 2022, https://doi.org/10.1007/s00170-021-08183-z

Emrecan Soylemez is currently an Associate Professor in Mechanical Engineering Department at Istanbul Technical University and has been a member since 2018. He is the director of the ITU Additive Manufacturing and Research Laboratory (EKAM). He received a B.S. degree in Mechanical Engineering from Istanbul Technical University, and M.S and Ph.D. at Carnegie Mellon University. His research focuses on metal AM processes, mainly binder jetting and fusion based powder bed processes. Understanding the process behavior, modeling and optimizing the process parameters are in his scope.